

Journal of Materials Chemistry A

Accepted Manuscript



This is an *Accepted Manuscript*, which has been through the Royal Society of Chemistry peer review process and has been accepted for publication.

Accepted Manuscripts are published online shortly after acceptance, before technical editing, formatting and proof reading. Using this free service, authors can make their results available to the community, in citable form, before we publish the edited article. We will replace this *Accepted Manuscript* with the edited and formatted *Advance Article* as soon as it is available.

You can find more information about *Accepted Manuscripts* in the [Information for Authors](#).

Please note that technical editing may introduce minor changes to the text and/or graphics, which may alter content. The journal's standard [Terms & Conditions](#) and the [Ethical guidelines](#) still apply. In no event shall the Royal Society of Chemistry be held responsible for any errors or omissions in this *Accepted Manuscript* or any consequences arising from the use of any information it contains.

Cite this: DOI: 10.1039/c0xx00000x

www.rsc.org/xxxxxx

ARTICLE TYPE

Efficient High Active Mass Paper-Based Energy-Storage Devices containing Free-standing Additive-less Polypyrrole-Nanocellulose Electrodes

Zhaohui Wang,^{*a} Petter Tammela,^b Peng Zhang,^b Maria Strømme,^{*b} Leif Nyholm^{*a}

Received (in XXX, XXX) Xth XXXXXXXXX 20XX, Accepted Xth XXXXXXXXX 20XX
DOI: 10.1039/b000000x

Free-standing and additive-free paper electrode containing up to 90 wt.% polypyrrole (PPy), and with PPy mass loadings up to 20 mg cm⁻², are made from PPy@nanocellulose and interconnecting PPy nanofibres for high-performance paper-based energy storage devices exhibiting close to theoretical energy densities and cell capacitances of about 1 F cm⁻² at current densities of 270 mA cm⁻².

The development of versatile energy storage devices has constituted the foundation for the unprecedented advancement of portable electronic system during the past two decades. To meet the needs of the next-generation electronic industry with high requirements on sustainability it is foreseen that an equally extraordinary advancement is necessary regarding the development of lightweight, inexpensive and environmentally-friendly high-performance energy storage devices.¹⁻⁸ State-of-the-art functional electrodes for energy storage devices generally share a common design in which carbon black additives and polymeric binders are included to provide electrical conduction and improved electrical contacts between the active materials and current collector, respectively.⁹⁻¹¹ Such additives, however, increase the weight of the electrode (typically by 10-40%) and also require additional processing steps in the manufacturing, which decrease the energy and power densities and increase the manufacturing cost of the storage devices. It should also be noted that while many of the high-performance electrode materials currently under development can be cycled at high rates and exhibit good gravimetric capacities, the total amount of electroactive material in these electrodes is often small. This is due to the fact that many of these materials are composed of a thin coating of an electroactive material on a more or less porous substrate, which, unfortunately, can render the use of these materials in energy storage devices difficult due to too low volumetric capacities, economical factors or technical problems associated with up-scaled production. Moreover, unrealistic energy densities and power densities are also sometimes reported, most likely due to problems associated with the determination of the amount of the small amounts of electroactive material. The search for sustainable, additive-free and inexpensive free-standing electrodes with high-active mass is therefore becoming one of the key challenges in the development of energy storage devices compatible with the next generation of electronic devices.

Conducting polymers, such as polypyrrole (PPy), polyaniline (PANI) and polythiophene are particularly interesting materials in the search for novel electrode materials due to their inherent fast redox switching, high conductivities, low weight and straightforward manufacturing processes which potentially could include biomass as the raw material.¹²⁻¹⁹ As has been described recently, nanocellulose fibres constitute highly appealing substrates for conducting polymers due to their ability to form mechanically robust and flexible structures when covered with the polymers.^{20, 21} In addition, cellulose is the most abundant biopolymer on earth and industrial processes for the manufacturing of nanocellulose fibres are also in the process of becoming established.^{22, 23} Composites in which thin conformal layer of PPy covers the individual cellulose nanofibres (hereafter referred to as PPy@nanocellulose) are particular interesting as a result of their high surface areas and charge capacities, and several attempts to construct sustainable energy storage devices based on such composites have therefore been described recently.^{13, 18, 24-27} It has been shown that PPy and cellulose based composites can be directly used as free-standing, additive-free high-performance electrodes in paper-based sustainable energy storage devices^{18, 21, 28} as well as for electrochemically controlled ion extraction.²⁹⁻³¹ Although attempts have been made,²⁷ it has, unfortunately, been difficult to further increase the mass loadings of these electrodes with the existing deposition approaches involving chemical or electrochemical polymerization of pyrrole (yielding PPy layers on the cellulose fibres with a thickness of only approximately 50 nm). New approaches to fabricate paper-based electrodes with higher mass loadings but with maintained microstructures would therefore provide a versatile means of obtaining increased capacities for low-cost and environmentally friendly energy-storage devices.

Herein, we present a novel approach in which the unique properties of high conductivity PPy@nanocellulose fibres is employed to fabricate free-standing binder- and carbon-additive-free electrodes containing as much as 90 wt.% PPy which give rise to PPy mass loadings of up to 20 mg cm⁻². We are not aware of any previous publications in which mass loadings and active masses of electroactive materials as high as these have been reported for paper-based electrode materials. The present concept relies on the integration of free-standing PPy nanofibres into a composite of PPy and nanocellulose, and unlike earlier reported

fabrication processes for PPy@nanocellulose fibre-based high-rate electrodes,^{32, 33} no polymer binders or carbon additives are required to ensure a high electrical conductivity and mechanical integrity of the electrodes. It is demonstrated that the novel composites can be used to fabricate environmentally friendly, symmetric supercapacitor cells operating in aqueous electrolytes with close to theoretical energy densities and cell capacitances of up to 1 F cm^{-2} (and specific capacitances of up to 96 F g^{-1}) at current densities of 270 mA cm^{-2} . As this novel approach also may be utilized to fabricate free-standing additive-less, high-performance electrodes based on other electroactive materials than PPy, it provides new possibilities for the preparation of tailor-made electric energy storage devices for a number of applications including medical devices, portable electronics, as well as for the management of existing and future intermittent renewable energy sources.

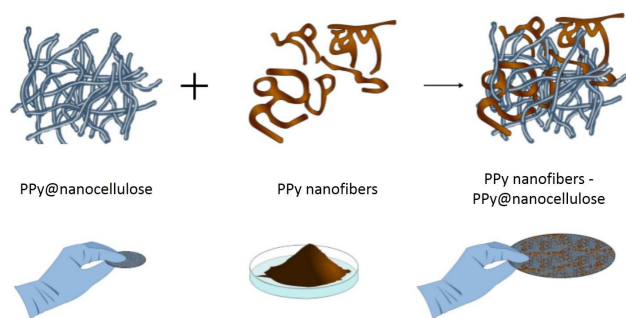


Fig. 1 Schematic illustration of the preparation of the present free-standing binder-free electrodes in which PPy nanofibres are integrate into a matrix of PPy@nanocellulose.

As is seen in **Fig. 1**, illustrating the electrode preparation strategy, interconnected PPy nanofibres were first synthesized and dispersed in water, essentially as previously described,³²⁻³⁴ while thin PPy coated cellulose nanofibres were synthesized separately by chemical polymerization.^{13, 21, 28} After mixing and subsequent filtration of the suspensions containing nanofibres of PPy and PPy@nanocellulose, respectively, paper-like electrodes, ready for use as electrodes in paper-based symmetric energy storage devices, were readily obtained (see the Experimental section, Supporting Information (SI)). This new and versatile approach has several advantages with respect to current state-of-the art methods since: i) the PPy@nanocellulose fibres serve both as the composite backbone material to obtain mechanically robust, free-standing paper-like electrodes and as a conducting binder facilitating the contact between the PPy nanofibres; ii) the inclusion of the intertwined PPy nanofibres yields electrodes with higher weight fractions of PPy (i.e. up to 90%) compared to for composites containing only PPy coated nanocellulose; iii) both the PPy nanofibres and the PPy coating on the nanocellulose fibres contribute to the charge storage capacity, yielding significantly increased mass loadings of the electroactive material; iv) the intertwined PPy nanofibres may facilitate electron transport by interconnecting the PPy coated nanocellulose fibres; and finally v) up-scaling may benefit from the industrial processes currently employed for paper making.

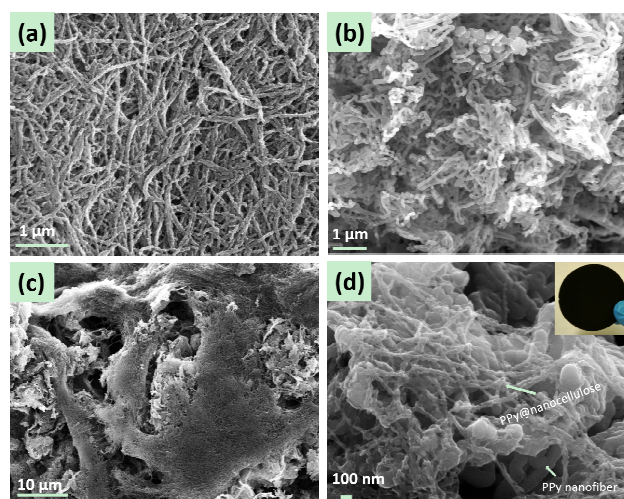


Fig. 2 SEM images for (a) PPy@nanocellulose, (b) interconnected PPy nanofibres and (c, d) PPy nanofibre-PPy@nanocellulose composites at different magnifications. The inset in panel d) shows a photograph of the paper-like composite obtained when mixing the PPy@nanocellulose and PPy nanofibres.

Fig. 2a displays a typical scanning electron microscopy (SEM) image of a PPy@nanocellulose composite, indicating the presence of an open, porous structure of intertwined fibres. Our previous transmission electron microscopy (TEM) studies have shown that the thickness of the PPy layer covering the nanocellulose fibres is $\sim 50 \text{ nm}$.¹³ A Fourier transform infrared (FTIR) spectrum for the nanofibres, confirming the presence of PPy, is shown in **Fig. S1** (SI). In **Fig. 2b** and **Fig. S2** (SI), it is seen that the PPy nanofibres exhibit a cross-linked structure with a fibre diameter of about 100 nm in good agreement with previous studies.^{32, 33} It should be noted that these PPy nanofibres are obtained in the form of a powder whereas a free-standing composite is obtained with the PPy@nanocellulose fibres. As is seen in **Fig. 2c** and **2d**, the combination of the latter two approaches gives rise to a new composite in which the PPy@nanocellulose fibres interconnect the PPy nanofibres giving rise to a 3D matrix, macroscopically appearing as a black glossy paper (cf. inset in **Fig. 2d**). According to nitrogen adsorption-desorption isotherms (**Fig. S3, SI**), the latter material exhibits a specific Brunauer–Emmett–Teller (BET) surface area of $40 \text{ m}^2 \text{ g}^{-1}$, corroborating the porous nature of the material visible in the SEM images. The surface area is, in fact, somewhat lower than those for the dry PPy ($48 \text{ m}^2 \text{ g}^{-1}$) and PPy@nanocellulose fibres ($72 \text{ m}^2 \text{ g}^{-1}$) indicating that the two types of fibres effectively infiltrate voids in each other's structure. The latter can be expected to promote the electrical contact between the constituents of the final composite.

Cyclic voltammetry (CV) experiments in a 2.0 M NaCl aqueous electrolyte, employing a three-electrode set-up, were carried out to evaluate the electrochemical properties of the novel composite electrode material depicted in **Fig. 2c** and **2d**. In these experiments, the potential window was specifically selected for each scan rate to compensate for the iR drop and to avoid PPy overoxidation by reversing the potential scan immediately prior to the onset of the overoxidation peak.²⁸ Voltammograms recorded at scan rates from 1 mV s^{-1} to 200 mV s^{-1} are shown in **Fig. 3a** whereas the oxidation charge capacities, obtained by

integration of the anodic peaks, are presented in **Fig. 3b**. It is seen that the specific capacity for the PPy nanofibre-PPy@nanocellulose electrodes was $\sim 218 \text{ C g}^{-1}$ (based on the electrode weight) for a scan rate of 5 mV s^{-1} which is comparable to - or even better than - those found for aerogel composites of nanofibrillated cellulose (NFC) and PPy,²¹ for PPy/graphite fiber composites³⁵ and for carbon fiber reinforced PPy@nanocellulose composites.²⁸ In addition, a specific capacity of $\sim 146 \text{ C g}^{-1}$ (based on the weight of electrode) could be maintained at the highest scan rate of 200 mV s^{-1} employed in the present study. This value is higher than the reported charge capacity for redox anion doped-PPy decorated cellulose (125 C g^{-1})³⁶ and and PPy-carbon fibre composites (126 C g^{-1} at 100 mV s^{-1}).³⁷ Here it should also be noted that the PPy-weight-based capacities often reported in the literature generally correspond to significantly lower values when normalised with respect to the total weight of the electrodes whereas this effect is small for the present electrodes composed of up to 90% of PPy.

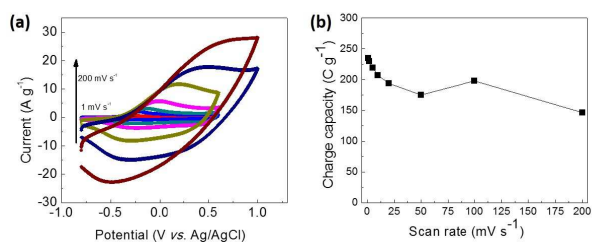


Fig. 3 (a) Cyclic voltammograms and (b) charge capacities for PPy nanofibre-PPy@nanocellulose composite electrodes obtained at scan rates from 1 to 200 mV s^{-1} . The displayed values have been normalized with respect to the total mass of the working electrodes.

To further investigate the electrochemical performance of the composites, two-electrode constant current charge/discharge experiments were carried out with symmetric energy storage devices. **Fig. 4a** and **4b** show galvanostatic charge/discharge curves recorded using current densities between 7 and 270 mA cm^{-2} (corresponding to 0.43 to 16.8 A g^{-1} based on the weight of one electrode). The chronopotentiograms in panel **4a** exhibit rather linear and symmetric shapes, in good agreement with the pseudocapacitive behaviour expected for surface confined redox reactions.³⁸ Note that the cut-off value for the charging step was set to 0.8 V in all experiments, whereas the actually measured cell voltages were somewhat higher than 0.8 V when very large charging currents were used (**Fig. 4b**). For current densities above $\sim 40 \text{ mA cm}^{-2}$, the effect of the iR drop is clearly visible and the resistance obtained from the iR drop of the discharge curves for a current density of 270 mA cm^{-2} was $\sim 1.4 \Omega$. This value is in good agreement with previously obtained values for PPy@nanocellulose based electrodes.²⁶ As was previously demonstrated the cell resistance can be decreased via an introduction of chopped carbon fibers (CCF) into the PPy-based electrodes.²⁸ We are not aware of any previous work in which additive-free conducting polymer paper-based electrode materials have been shown to be compatible with current densities as high as these (i.e. 270 mA cm^{-2} or 16.8 A g^{-1}), yielding charging times of about 1.2 s . Although Razaq *et al.*²⁸ reported the successful employment of current densities of 99 mA cm^{-2} or 31 A g^{-1} (PPy), the PPy@nanocellulose composite electrodes used in that study

contained up to 47% CCF as an additive to decrease the cell resistance. As no such additives were used in the present case, the PPy nanofibre- PPy@nanocellulose electrodes are clearly very promising for applications in which both high energy density and power density are required. As will be described below, the energy densities were in fact found to be close to the theoretical values for symmetric PPy-based energy storage devices.

Although porous 3D graphene electrodes³⁹ as well as PANI films coated on graphitic petal electrodes³⁸ have been shown to be compatible with current densities of up to 100 A g^{-1} , the area-normalized current densities for these electrodes were in fact only about 120 mA cm^{-2} due to relative low mass loadings. As the latter type of electrodes typically have mass loadings of $\sim 1 \text{ mg cm}^{-2}$ due to the use of thin electroactive layers, relatively small capacities (i.e. $\sim 0.06 \text{ C cm}^{-2}$ for a 3D graphene electrode³⁹), are generally obtained despite the reported high areal capacitances. The device capacity of 0.324 C cm^{-2} (for a mass loading of 20 mg cm^{-2}) obtained for the present symmetric device at a current density of 270 mA cm^{-2} and the corresponding value of 1.18 C cm^{-2} obtained for a current density of 1.35 mA cm^{-2} thus represent significant progress with respect to the previously described symmetric and asymmetric energy storage devices investigated at significantly lower current densities.^{39, 40}

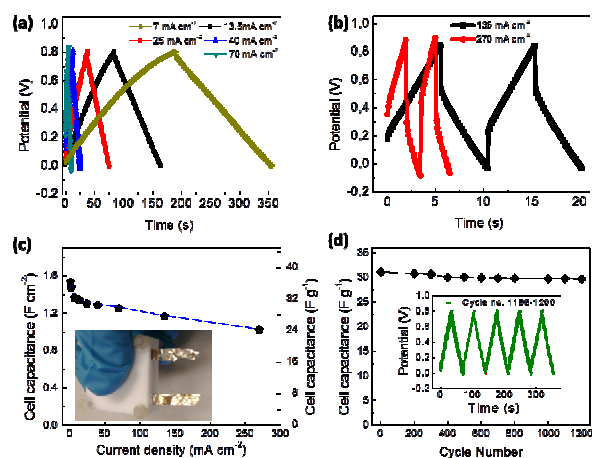


Fig. 4 (a, b) Galvanostatic charge/discharge curves for symmetric two-electrode devices obtained at different current densities. (c) Cell capacitances vs. current density obtained from the measurements in panels (a) and (b). The inset in (c) depicts one of the tightly sealed cells. (d) Cell capacitances vs. cycle number obtained from a 1200 cycle charge/discharge cycling test performed with a current density of 25 mA cm^{-2} . The last five charge/discharge cycles are displayed in the inset in (d). The capacitance values on the right-hand axis of panel (c) and the left-hand axis of panel (d) have been normalized using the total mass of both electrodes.

The gravimetric cell capacitances and area-normalized cell capacitances, extracted from the discharge curves obtained for charge/discharge current densities between 1.35 and 270 mA cm^{-2} with respect to the mass of both electrodes, are presented in **Fig. 4c**. For a current density of 1.35 mA cm^{-2} , the gravimetric cell and area-normalized cell capacitances were thus 36.3 F g^{-1} (based on the weight of both electrodes) and 1.54 F cm^{-2} , respectively, clearly exceeding the values (of 21 F g^{-1} and 0.48 F cm^{-2}) previously reported for devices based on PPy-based paper electrodes.²⁸ We are not aware of any previous reports

demonstrating similar capacities for an energy storage device composed of PPy-based electrode. A charge capacity of 1.5 C cm^{-2} , has, on the other hand, been obtained with a PPy/porous graphite fiber composite³⁵ at a scan rate of 20 mV s^{-1} but since the corresponding electrode and cell area based capacities were not stated it is difficult to compare these values with the ones obtained for the present composites.

As is seen in Fig. 4c, the gravimetric and area-normalized cell capacitances decreased with increasing current densities but still remained relatively stable at high current densities. For a current density of 270 mA cm^{-2} (i.e. 16.8 A g^{-1}), the area-normalized cell capacitance was still close to 1 F cm^{-2} which still is significantly higher than the values recently presented for PPy- or graphene-based supercapacitors obtained at significantly lower current densities (i.e. flexible graphene-PPy nanofiber membrane⁴¹ (0.175 F cm^{-2} at 10 mV s^{-1}), MnO_2 /reduced graphene oxide paper⁴⁰ (0.113 F cm^{-2} at 10 mA g^{-1}), conductive wrapped graphene/ MnO_2 ⁴² (0.5 F cm^{-2} at 0.1 mA cm^{-2})). The present paper-based electrodes have a significantly higher mass loading of $\sim 20 \text{ mg cm}^{-2}$, which in fact matches the standard mass loading for electrodes given by Simon and Gogotsi⁴³ well. A high electrode mass loading is clearly imperial when it comes to storing significant amounts of energy in real energy storage devices.

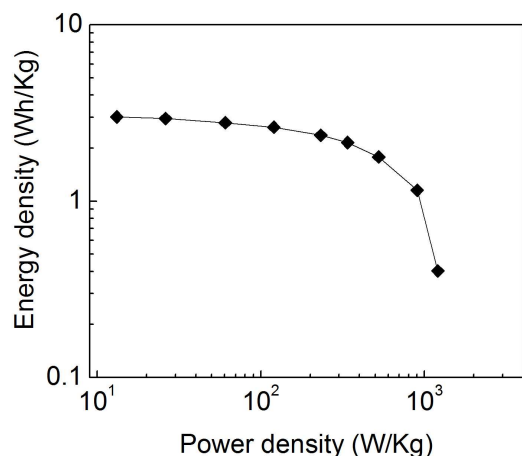


Fig. 5 Ragone plot for the symmetric energy storage device containing two PPy nanofibre-PPy@nanocellulose paper electrodes. The energy and power density values have been normalized with respect to the weight of both electrodes.

Based on the device data in Fig. 4a and 4b, an energy density of 3.0 Wh kg^{-1} and a power density of 1.2 kW kg^{-1} (corresponding to 0.75 Wh L^{-1} and 0.3 kW L^{-1} , based on the mass of both electrodes) were obtained after normalization with respect to the weight of both electrodes (see Fig. 5). These values are higher than those for the recently described CCF reinforced PPy-based paper electrodes (i.e., 0.61 Wh kg^{-1} and 0.95 kW kg^{-1} , based on twice the weight of the smaller electrode).²⁸ The energy density obtained from the voltammetric experiments presented in Fig. 3 are, on the other hand, significantly higher, i.e. 18 Wh kg^{-1} when normalised with respect to the electrode weight, and 20 Wh kg^{-1} after normalisation with respect to the PPy weight. Energy and power densities of up to 49.5 Wh kg^{-1} and 12 kW kg^{-1} ,⁴⁴ have likewise recently been reported for PPy deposited on monolithic

carbon based on one-volt three-electrode test and normalization with respect to the PPy weight. Since it is well-known¹⁵ that the values for a symmetric two-electrode device (normalised with the weight of both electrodes) should be four times lower than those obtained in the corresponding three-electrode experiments, the present data clearly illustrate the problems associated with comparisons of three-electrode and device data. Since the theoretical capacity for PPy is 360 C g^{-1} , assuming a doping degree of 25% at $+0.6 \text{ V vs. Ag/AgCl}$ (a potential which typically is employed to avoid overoxidation effects^{15, 26, 45}), the attainable theoretical energy density for a PPy electrode charged to $+0.6 \text{ V vs. Ag/AgCl}$ in a three-electrode experiment can be estimated to be 30 Wh kg^{-1} (PPy) as is described in the SI. As the experimental value corresponded to about 67% of the theoretical value, the energy density of the present device can consequently only be further increased by a factor of 1.5. It is also evident that specific capacitances, energy densities and power densities exceeding about 600 F g^{-1} , 30 Wh kg^{-1} (PPy) and 110 kW kg^{-1} (PPy) (assuming a discharge time of 1 s and an energy density of 30 Wh kg^{-1} (PPy)), respectively, are very unlikely to be obtained for PPy-based electrodes charged to $+0.6 \text{ V}$ in three-electrode experiments. Although the energy and power densities could be increased further by charging to a higher potential this would significantly increase the influence of degradation due to overoxidation, particularly when the device is stored in its charged state.^{15, 26, 45}

For a symmetrical two-electrode PPy device charged to 0.8 V (in which each electrode is charged by 0.4 V), a theoretical energy density of 3.3 Wh kg^{-1} (PPy) can likewise be obtained after normalisation with respect to the PPy weight of both electrodes. This value, which is approximately nine times smaller than that for the corresponding three-electrode experiment (see the SI), is comparable to the energy density of 3.0 Wh kg^{-1} obtained for the device. This indicates that the present device in fact operated close to its theoretical energy density limit in good agreement with the previous discussion based on the voltammetric data. The theoretical power density for the device can analogously be estimated to about 10 kW kg^{-1} (PPy) assuming a discharge time of 1.2 s, a value which should be compared with the obtained value of 1.2 kW kg^{-1} obtained using a current density of 270 mA cm^{-2} . Since the corresponding experimental value was 13 W kg^{-1} for a current density of 1.35 mA cm^{-2} in very good agreement with the corresponding theoretical value of 14 W kg^{-1} (for a discharge time of 877 s) it is clear that the full capacity of the device could be utilised on a sufficiently long time scale and that difference between the theoretical and experimental values increased with increasing current density. This is in good agreement with the expected behaviour for composites with high mass loadings since recent findings⁴⁶ clearly demonstrate that the mass transport of the counter ions within the porosities of these composites become limiting when the time scale of the experiment decreases. As these effects are less likely to be observed for very thin PPy films (containing only very small amounts of active material) it is immediately evident that the theoretical power densities for PPy-based electrodes only are can be reached for electrodes with very low mass loadings (which unfortunately are of little interest for use in energy storage devices due to their limited charge storage

capacities). In this light, the power density of 1.2 kW kg^{-1} , obtained for the present device containing electrodes with mass loadings of up to 20 mg cm^{-2} , is very promising.

The results of galvanostatic cycling stability experiments involving an analogous symmetric device containing PPy nanofibre-PPy@nanocellulose paper electrodes are shown in **Fig. 4d**. It is seen that a cell capacitance of 1.32 F cm^{-2} was obtained for a current density of 25 mA cm^{-2} (i.e. 1.56 A g^{-1}) and that a capacitance drop of about 5 % was found after 1200 charge/discharge cycles, indicating good electrochemical stability. The charging time of $\sim 36 \text{ s}$ yields a charge capacity of $\sim 0.9 \text{ C cm}^{-2}$ and the capacity retention was found to be almost 100 % during the 1200 charge/discharge cycles (**Fig. S4**, SI). As is seen from the insert in **Fig. 4d** depicting the charge/discharge voltage profiles for the last five cycles, the coulombic efficiency was also very close to 100 %. The fact that the obtained cell capacitance of 31 F g^{-1} is significantly larger than the previously obtained capacitances for PPy@nanocellulose based devices is a direct result of the fact that the composite contained about 90 % of PPy as compared to about 65-70 % for the previous devices.

Conclusions

In summary, the present approach constitutes a new, versatile and straightforward method for the fabrication of free-standing PPy nanofibre-PPy@nanocellulose composites yielding electrodes with high active mass ratios and high mass loadings. The unique architecture of this paper-based material enables efficient use of pseudocapacitive PPy nanomaterials for charge storage with facilitated transport of both counter ions and electrons yielding close to theoretical energy densities. This facilitates the manufacturing of efficient paper-based energy storage devices with high cell capacitances, excellent rate capabilities and remarkable cycling performances. The approach for the manufacturing of free-standing paper electrode presented in this work can most likely also be extended to include a variety of other materials (i.e. LiFePO_4 , see **Fig. S5**, SI), as well as energy conversion and storage applications. The present type of low-cost, lightweight, and high-performance electrodes based on abundant and environment-friendly materials (which also can be up-scaled for industrial applications) hence offer great promise for use in advanced energy storage devices in which conventional devices cannot be used due to e.g. demands regarding conformability, safety, low-cost or environmental friendliness.¹⁵

Acknowledgements

The Swedish Foundation for Strategic Research (SSF) (grant RMA-110012), The Swedish Energy Agency (project SwedGrids), The Carl Trygger Foundation and the European Institute of Innovation and Technology under the KIC InnoEnergy NewMat and electrical energy storage project, are gratefully acknowledged for financial support of this work.

Notes and references

^a Department of Chemistry-The Ångström Laboratory, Uppsala University, Box 538, SE-751 21 Uppsala, Sweden, E-mail: zhaohui.wang@kemi.uu.se leif.nyholm@kemi.uu.se;

^b Nanotechnology and Functional Materials, Department of Engineering Sciences, The Ångström Laboratory, Uppsala University, Box 534, SE-751 21 Uppsala, Sweden, E-mail: maria.stromme@angstrom.uu.se;
† Electronic Supplementary Information (ESI) available: [details of any supplementary information available should be included here]. See DOI: 10.1039/b000000x/

1. M. S. Whittingham, *Chem. rev.*, 2004, **104**, 4271-4302.
2. M. Armand and J. Tarascon, *Nature*, 2008, **451**, 2-7.
3. C. Liu, F. Li, L.-P. Ma and H.-M. Cheng, *Adv. mater.*, 2010, **22**, E28-62.
4. B. Scrosati and J. Garche, *J. Power Sources*, 2010, **195**, 2419-2430.
5. V. L. Pushparaj, M. M. Shaijumon, A. Kumar, S. Murugesan, L. Ci, R. Vajtai, R. J. Linhardt, O. Nalamasu and P. M. Ajayan, *Proc. Natl. Acad. Sci. U. S. A.*, 2007, **104**, 13574-13577.
6. B. Dunn, H. Kamath and J. M. Tarascon, *Science*, 2011, **334**, 928-935.
7. L. Yuan, X. Xiao, T. Ding, J. Zhong, X. Zhang, Y. Shen, B. Hu, Y. Huang, J. Zhou and Z. L. Wang, *Angew. Chem.*, 2012, **124**, 5018-5022.
8. Q. Zhong, J. Zhong, B. Hu, Q. Hu, J. Zhou and Z. L. Wang, *Energy Environ. Sci.*, 2013, **6**, 1779-1784.
9. D.-H. Ha, M. A. Islam and R. D. Robinson, *Nano Letters*, 2012.
10. G. Q. Zhang, H. B. Wu, H. E. Hoster, M. B. Chan-Park and X. W. Lou, *Energy Environ. Sci.*, 2012, **5**, 9453.
11. S. Leijonmarck, A. Cornell, G. Lindbergh and L. Wågberg, *J. Mater. Chem A*, 2013, **1**, 4671-4677.
12. S. Ghosh, J. Rasmusson and O. Inganas, *Adv. Mater.*, 1998, **10**, 1097-+.
13. G. Nyström, A. Razaq, M. Stromme, L. Nyholm and A. Mihranyan, *Nano Lett*, 2009, **9**, 3635-3639.
14. P. Novák, K. Müller, K. Santhanam and O. Haas, *Chem. Rev.*, 1997, **97**, 207-282.
15. L. Nyholm, G. Nyström, A. Mihranyan and M. Strømme, *Adv. Mater.*, 2011, **23**, 3751-3769.
16. G. Milczarek and O. Inganas, *Science*, 2012, **335**, 1468-1471.
17. E. Frackowiak, V. Khomenko, K. Jurewicz, K. Lota and F. Béguin, *J. Power Sources*, 2006, **153**, 413-418.
18. L. Yuan, B. Yao, B. Hu, K. Huo, W. Chen and J. Zhou, *Energy Environ. Sci.*, 2012, **6**, 470.
19. B. Yao, L. Yuan, X. Xiao, J. Zhang, Y. Qi, J. Zhou, J. Zhou, B. Hu and W. Chen, *Nano Energy*, 2013, **2**, 1071-1078.
20. M. Pääkkö, J. Vapaaauori, R. Silvennoinen, H. Kosonen, M. Ankerfors, T. Lindström, L. A. Berglund and O. Ikkala, *Soft Matter*, 2008, **4**, 2492-2499.
21. D. O. Carlsson, G. Nyström, Q. Zhou, L. A. Berglund, L. Nyholm and M. Strømme, *J. Mater. Chem*, 2012, **22**, 19014.
22. D. Klemm, F. Kramer, S. Moritz, T. Lindström, M. Ankerfors, D. Gray and A. Dorris, *Angew. Chem. Int. Ed.*, 2011, **50**, 5438-5466.
23. L. Hu, G. Zheng, J. Yao, N. Liu, B. Weil, M. Eskilsson, E. Karabulut, Z. Ruan, S. Fan, J. T. Bloking, M. D. McGehee, L. Wågberg and Y. Cui, *Energy Environ. Sci.*, 2013, **6**, 513.
24. L. Jabbour, R. Bongiovanni, D. Chaussy, C. Gerbaldi and D. Beneventi, *Cellulose*, 2013.
25. G. Nyström, A. Mihranyan, A. Razaq, T. Lindström, L. Nyholm and M. Strømme, *J. Phys. Chem. B*, 2010, **114**, 4178-4182.
26. G. Nyström, M. Strømme, M. Sjödin and L. Nyholm, *Electrochim. Acta*, 2012, **70**, 91-97.

27. H. Olsson, D. O. Carlsson, G. Nyström, M. Sjödin, L. Nyholm and M. Strømme, *J. Mater. Sci.*, 2012, **47**, 5317-5325.
28. A. Razaq, L. Nyholm, M. Sjödin, M. Strømme and A. Mihranyan, *Adv. Energy Mater.*, 2012, **2**, 445-454.
- 5 29. N. Ferraz, D. O. Carlsson, J. Hong, R. Larsson, B. Fellström, L. Nyholm, M. Strømme and A. Mihranyan, *J. R. Soc. Interface*, 2012, **9**, 1943-1955.
30. K. Gelin, A. Mihranyan, A. Razaq, L. Nyholm and M. Strømme, *Electrochim. Acta*, 2009, **54**, 3394-3401.
- 10 31. A. Mihranyan, L. Nyholm, A. E. G. Bennett and M. Strømme, *J. Phys. Chem. B*, 2008, **112**, 12249-12255.
32. Z. Wang, X. Xiong, L. Qie and Y. Huang, *Electrochimica Acta*, 2013, **106**, 320-326.
33. Z. Wang, L. Qie, L. Yuan, W. Zhang, X. Hu and Y. Huang, *Carbon*,
15 2013, **55**, 328-334.
34. L. Qie, W. M. Chen, Z. H. Wang, Q. G. Shao, X. Li, L. X. Yuan, X. L. Hu, W. X. Zhang and Y. H. Huang, *Adv Mater*, 2012, **24**, 2047-2050.
35. B. Coffey, P. Madsen, T. Poehler and P. Searson, *J Electrochem. Soc.*, 1995, **142**, 321-325.
- 20 36. S. Y. Kim, J. Hong and G. T. R. Palmore, *Synth. Met.*, 2012, **162**, 1478-1481.
37. R. A. Davoglio, S. R. Biaggio, N. Bocchi and R. C. Rocha-Filho, *Electrochim. Acta*, 2013, **93**, 93-100.
38. G. Xiong, C. Meng, R. G. Reifengerger, P. P. Irazoqui and T. S.
25 Fisher, *Adv. Energy Mater.*, 2013, DOI: 10.1002/aenm.201300515.
39. *Adv. Mater.*, 2013, **25**, 2474-2480.
40. A. Sumboja, C. Y. Foo, X. Wang and P. S. Lee, *Adv. Mater.*, 2013,
25, 2809-2815.
41. J. Zhang, P. Chen, B. H. Oh and M. B. Chan-Park, *Nanoscale*, 2013,
30 **5**, 9860-9866.
42. G. Yu, L. Hu, N. Liu, H. Wang, M. Vosgueritchian, Y. Yang, Y. Cui and Z. Bao, *Nano Lett*, 2011, **11**, 4438-4442.
43. Y. Gogotsi and P. Simon, *Science*, 2011, **334**, 917-918.
44. Y. Wang, S. Tao, Y. An, S. Wu and C. Meng, *J. Mater. Chem. A*,
35 2013.
45. H. Olsson, G. Nyström, M. Strømme, M. Sjödin and L. Nyholm, *Electrochem. Commun.*, 2011, **13**, 869-871.
46. D. O. Carlsson, A. Mihranyan, M. Strømme and L. Nyholm, *RSC Adv.*, 2014, DOI: 10.1039/c3ra47588c.

40

The table of contents

A novel approach is employed to fabricate free-standing and additive-free paper electrodes containing up to 90 wt.% polypyrrole (PPy), and with PPy mass loadings up to 20 mg cm^{-2} , which demonstrates excellent charge storage performance for paper-based energy storage devices.

